Removal of Pb(II) and Cd(II) from aqueous solution using alkaline-modified pumice stone powder (PSP): equilibrium, kinetic, and thermodynamic studies

Vivian JONASI, Kaina MATINA, Upenyu GUYO*
Department of Chemical Technology, Faculty of Science and Technology, Midlands State University,
Gweru, Zimbabwe

Abstract: Adsorption processes of Cd(II) and Pb(II) from aqueous solutions onto pumice stone powder (PSP) were investigated in batch mode. The influences of solution pH, contact time, adsorbent dosage, initial metal (M) concentration, and temperature on adsorption process were investigated. The kinetic and isotherm data were analysed using different model equations. The adsorption process was consistent with the Langmuir model for both metal ions with high R^2 and low χ^2 values for both Pb(II) and Cd(II). The maximum monolayer adsorption capacities were 28.09 and 27.17 mg g^{-1} for Pb(II) and for Cd(II), respectively. The pseudo-second order kinetic model explained the kinetic data as evidenced by the calculated q_e (cal) values (10.42 mg g^{-1} for Pb(II) and 2.62 mg g^{-1} for Cd(II)) agreeing with the experimental values (9.24 mg g^{-1} for Pb(II) and 2.49 mg g^{-1} for Cd(II)). Consequently, the present study demonstrated that PSP could be utilised in adsorptive removal of Cd(II) and Pb(II) ions from aqueous solutions.

Key words: Removal, pumice stone powder, Cd(II), Pb(II), kinetics

1. Introduction

The increase in population growth and industrialisation has resulted in deterioration of both surface and ground water. The growth of metal use in industries has culminated in significant amounts of toxic heavy metals being deposited into the environment causing biosphere poisoning.[1] Heavy metal pollution of water is mainly due to discharges from electroplating metal and finishing industries.[2] Some of these metallic pollutants can be used as essential nutrients for both plants and animals but only if they are within the tolerance limits.[3] Removal of heavy metals is of great importance especially in industrial aquatic effluents. Metals such as cadmium, lead, chromium, and mercury are toxic to aquatic flora, animals, and humans if they exceed their tolerance limit.[4] Exposure to these metal effluents can be in form of gaseous emissions, aqueous deposits, and solid effluents. Of these metal sources, aqueous mediums are the greatest source of pollution.

Long-term effects of Cd(II) in humans such as hypertension, renal dysfunction, lung damage and hepatic injury, diarrhoea, and being teratogenic and short term effects such as vomiting, nausea, and cramps have been reported.[5−7] The maximum permissible concentration of Cd(II) in drinking water is 5 ppb according to the World Health Organization (WHO).[8] Pb(II) is nonbiodegradable and exposure to it for long may cause semipermanent brain damage, retardation, mental disturbance, and liver damage.[9−13] The WHO recommended that the maximum permissible amount of Pb(II) in drinking water should not exceed 0.01 mg L^{-1}.[14] The

*Correspondence: upguyo@gmail.com

Environmental Protection Agency's permissible Pb(II) level in wastewaters is 0.05 mg L^{-1}.[15] Hence, it is sensible to comply with the recommended limits before disposing wastewaters into major sinks to safeguard the environment and human health.

Metal removal from these areas has been subject to research and various methods have been developed so as to alleviate this threat to the environment. While heavy metal removal from waste effluent can be done by conventional processes such as solvent extraction, chemical precipitation, membrane technology, ion exchange, flotation, and coagulation each treatment process has its inherent limitations.[16] As efficient as these methods are, there is need for invention of cost effective alternative methods. Of these alternative methods, adsorption is one of the most cost effective methods for removal of the heavy metal ions in aqueous media.[1,17] Adsorption has several advantages over other processes such as a wide range of target pollutants, high adsorption capacity, and possibly selective adsorbent. There is increased interest among researchers towards the development of adsorbents that can be used as alternatives for commercial adsorbents.

Activated carbon has been widely used due to its large surface area, surface reactivity, and high adsorption capacity.[18] However, its expensive production cost makes it economically inefficient; thus there is a need for alternative adsorbents. The search for new alternative cost-effective adsorbents that have good metal capacities has increased and this has resulted in the discovery of cheaper adsorbents such as fly ash, coal, wool wastes, silica gel, agricultural wastes, clay minerals, and wood wastes.[3] These materials can be utilised as sorbents with little processing, thus assisting its economic value and assisting the industries to reduce costs of waste disposal and thus provide activated carbon alternatives.[1]

Pumice is one of the materials that can be employed in removing pollutants such as metals from water bodies or aqueous solutions.[1] Pumice is a very light, highly porous volcanic stone with a microporous structure, which gives it a high surface area.[19] Pumice stone has a basic or acidic character and high silica content, making it abrasive. High porosity and its richness in alumina and silica makes volcanic pumice rock a promising and potential candidate as an adsorbent.[17] The highly porous structure of pumice gives it a large surface area, which avoids the preliminary calcination step, which consumes large amounts of energy, and it can float in water due to its low density.[19] Research done on pumice has shown that it is ideal for impregnated metals on surface and thus can be used for removal of recalcitrant pollutants such as heavy metals. Pumice has a large proportion of silica sites, which gives it a negatively charged surface, and it has a large number of open sites, which allow water and ions to move in and out of the crystal structure. It also has a structure that enables molecules and ions to move and reside within the overall framework as the structure contains open chains allowing ions and water to travel into and out of the crystal structure.[4] Pumice rock is so light such that it floats on water and has proved to be effective in phosphate ion removal from water. However, to improve its absorption properties, pumice can be acidified to reduce negative charges on the adsorbent surface.[1,3]

The focus of this present study was to explore the applicability and feasibility of adsorption of Pb(II) and Cd(II) ions onto alkaline-modified pumice stones powder. The investigation was conducted through batch adsorption experiments with solution pH, contact time, adsorbent dosage, initial metal concentration, and concentration of the medium as independent variables.

2. Results and discussion

2.1. Effect of sorption parameters

2.1.1. Effect of pH

The solution pH affects metal adsorption onto an adsorbent.[20] The H^+ ions strongly compete with the adsorbate. The results of pH investigations are presented in Figure 1. The adsorption efficiency was minimum (47.4% for Pb(II) and 52.7% for Cd(II)) at pH 2.0. At low pH there is electrostatic repulsion between M^{2+} and H^+ ions. The majority of the binding sites are filled by H^+. The adsorption removal increased from 47.4% to 92.50% and 52.7% to 88.53% for Pb(II) and Cd(II) at pH 2.0–5.0, respectively. The slight decrease in adsorption of M(II) ions after pH 5 was perhaps as a result of formation of $M(OH)_2$ and soluble hydroxyl complexes such as MOH^+, aqueous $M(OH)_2$, and $M(OH)^{3-}$. Moreover, the adsorbent perhaps deteriorated with accumulation of M(II) ions making binding to adsorption sites impossible. Further adsorption experiments were carried at an optimum pH 5.0.
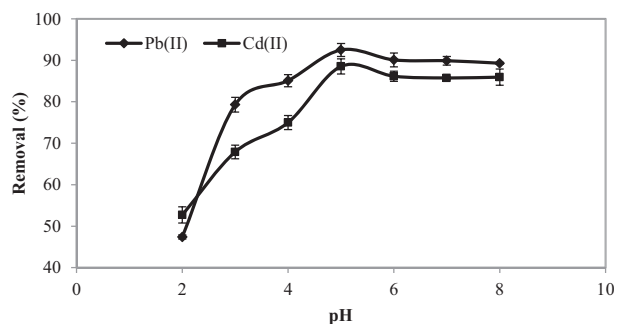

Figure 1. Effect of pH on Pb(II) and Cd(II) adsorption ($C_0 = 30$ mg L^{-1}, PSP dosage = 0.2 g, t = 120 min; *error bar* ±SD; and n = 3).

2.1.2. Effect of adsorbent dosage

The adsorbent dosage in adsorption studies determines the capacity of an adsorbent for a specified initial concentration.[21] The effect of PSP dosage on the uptake of Pb(II) and Cd(II) is shown in Figure 2. The adsorbent dosage profiles show an increase in the removal of metal ions with increase in dosage but beyond 0.3 g the percentage removal becomes almost constant due to reduction in the concentration gradient of the M(II) ions between the adsorbate and adsorbent. The initial increase in percentage removal of M(II) ions from solution might be due to the increased number of exchangeable open sites for adsorption. The maximum removal percentages of Pb(II) and Cd(II) from aqueous solutions were 96.70% and 86.17%, respectively.

2.1.3. Effect of contact time

The effects of contact time on the percentage removal of Pb(II) and Cd(II) ions from aqueous solution are presented in Figure 3.

The profile plots show the percentage removal increasing with increase in time, reaching a maximum of 92.39% for Pb(II) after 100 min and 82.69% for Cd(II) after 140 min. Adsorption efficiency was fast in the first 100 min. This can be attributed to availability of vacant larger surface area binding sites. Beyond the optimum, a further increase in contact time showed no apparent effect on metal ions percentage removal.
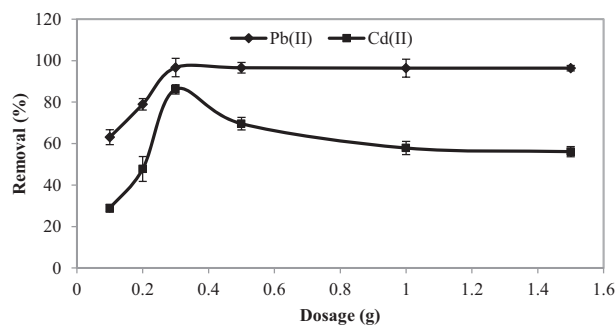
Figure 2. Effect of PSP dosage on Pb(II) and Cd(II) adsorption (pH = 5, $C_0 = 10$ mg L^{-1}, t = 120 min; *error bar* ±SD; and n = 3).
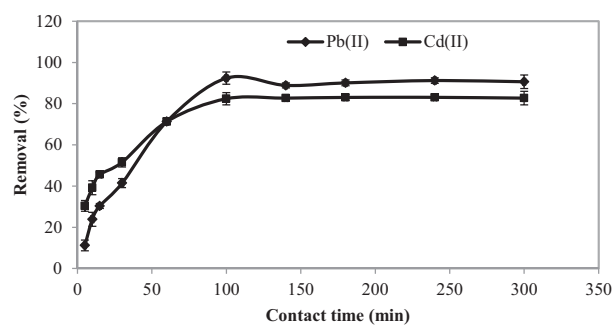
Figure 3. Effect of contact time on Pb(II) and Cd(II) adsorption (pH = 5, $C_0 = 10$ mg L^{-1}, PSP dosage = 0.3 g, *error bar* ±SD; and n = 3).

2.1.4. Effect of initial metal concentration

The efficiency and feasibility of an adsorption process also depend on concentration of aqueous metal ions. The influence of initial concentration on adsorption process was investigated within the concentration range 10–50 mg L^{-1} (Figure 4). There was a notable decrease in the removal of M(II) ions from 96.25% to 69.69% for Pb(II) and from 90.05% to 43.62% for Cd(II) ions as the initial concentration of the metal ions in solution was increased from 10 to 50 mg L^{-1}. At lower concentrations, most of the metal ions in solution interact with the adsorbent active sites and hence a higher percentage removal.[2] As the initial concentration is increased, the active sites become saturated and most of the metal ions remain unadsorbed.

2.1.5. Effect of temperature

The adsorption of M(II) on PSP was investigated with respect to temperature in the range of 20–50 °C (Figure 5). The adsorption efficiency of the adsorbent increased for both metal ions with increase in temperature up to 50 °C, showing endothermic behaviour of the sorption process. The increase in aqueous media temperature enhances the interaction of metal ions with adsorbent as the activation energy barrier for adsorption process is overcome. A temperature of 20 °C was however employed for further adsorption studies.
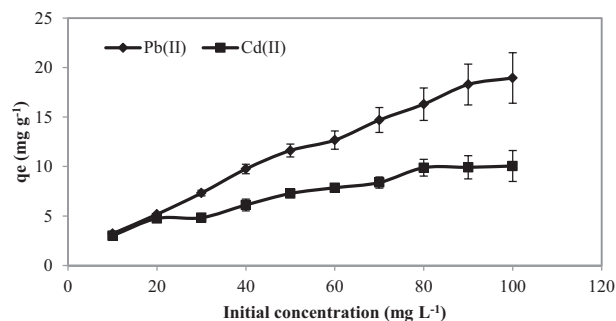

Figure 4. Effect of initial concentration on Pb(II) and Cd(II) adsorption (pH = 5, PSP dosage = 0.3 g, t = 100 min; *error bar* ±SD; and n = 3).
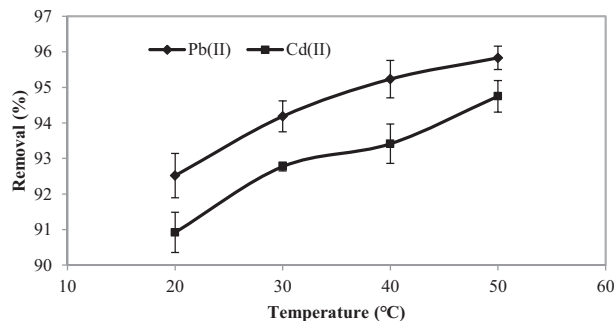
Figure 5. Effect of solution temperature on Pb(II) and Cd(II) adsorption (pH = 5, PSP dosage = 0.3 g, $C_0 = 10$ mg L^{-1}, t = 100 min; *error bar* ±SD; and n = 3).

3. Adsorption isotherms

The nature of the interaction between the adsorbate and adsorbent is determined by adsorption isotherms. In the current study, the Langmuir[22] and Freundlich[23] isotherms were applied to the experimental data.

The convergent linear form of the Temkin isotherm is expressed as

$$q_e = B_1 ln K_T + B_1 ln C_e, \tag{1}$$

where $B_1 = \frac{RT}{b}$, T is the absolute temperature (Kelvin), and R is the universal gas constant (J mol^{-1} K^{-1}). b is the Temkin constant related to the heat of adsorption and K_T is the equilibrium binding constant (L mg^{-1}) corresponding to the maximum binding energy. The Temkin model had lower coefficients of determinations at the four temperatures relative to other investigated models (Table 1). Hence, it could be inferred that the removal process was better modelled by monolayer compared to multilayer adsorption.

Table 1. Isotherm parameters.

Isotherm	Parameter	Pb(II)				Cd(II)			
	T(°C)	20	30	40	50	20	30	40	50
Langmuir	q_{max} (mg g^{-1})	28.09	23.20	19.13	25.25	15.36	16.58	17.15	27.17
	b (L mg^{-1})	0.040	0.052	0.120	0.056	0.030	0.028	0.026	0.008
	χ^2	107.90	73.23	33.87	25.51	46.90	53.35	60.53	164.63
	R^2	0.976	0.988	0.966	0.989	0.987	0.988	0.989	0.990
Freundlich	K_F (mg g^{-1})	2.160	1.970	3.250	2.280	1.320	1.320	1.200	2.930
	n	1.760	1.730	2.160	1.740	2.030	1.960	1.870	1.280
	χ^2	505.79	539.15	303.49	513.270	303.83	339.68	380.15	50.66
	R^2	0.91	0.986	0.987	0.985	0.962	0.965	0.970	0.988
Temkin	b	420.21	416.17	489.90	396.72	681.72	629.99	608.09	519.51
	K_T (L mg^{-1})	2.230	2.640	1.370	2.280	4.030	4.200	4.640	10.270
	R^2	0.903	0.948	0.933	0.970	0.969	0.971	0.974	0.962

The linearized form of the Langmuir isotherm model is given as

$$\frac{1}{q_e} = \frac{1}{q_{max}} + \left(\frac{1}{bq_{max}}\right)\frac{1}{C_e} \tag{2}$$

where q_e is the amount of metal ions adsorbed at equilibrium, q_{max} is the adsorption capacity (mg g^{-1}), C_e (mg L^{-1}) is the equilibrium concentration, and b is the equilibrium Langmuir constant. q_{max} and b (Table 1) were estimated from the intercept and slope of a plot of $1/q_e$ versus $1/C_e$ (Figure 6a), respectively.

The linearized form of the Freundlich adsorption isotherm model is given by

$$\ln q_e = \ln K_F + \frac{1}{n}\ln C_e, \tag{3}$$

where q_e (mg g^{-1}) is the amount of M(II) ion adsorbed at equilibrium, K_F (mg g^{-1}) is the adsorption capacity, n is the adsorption intensity and C_e (mg L^{-1}) is the concentration at equilibrium. n and K_F were estimated from the slope and intercept of plot of ln q_e versus ln C_e (Figure 6b), respectively. The values of n (Table 1) were found to be 1.76, 1.73, 2.16, and 1.74 at 20, 30, 40, and 50 °C, respectively, for Pb(II) and 2.03, 1.96, 1.20, and 1.28 at 20, 30, 40, and 50 °C, respectively, for Cd(II), indicating favourable and
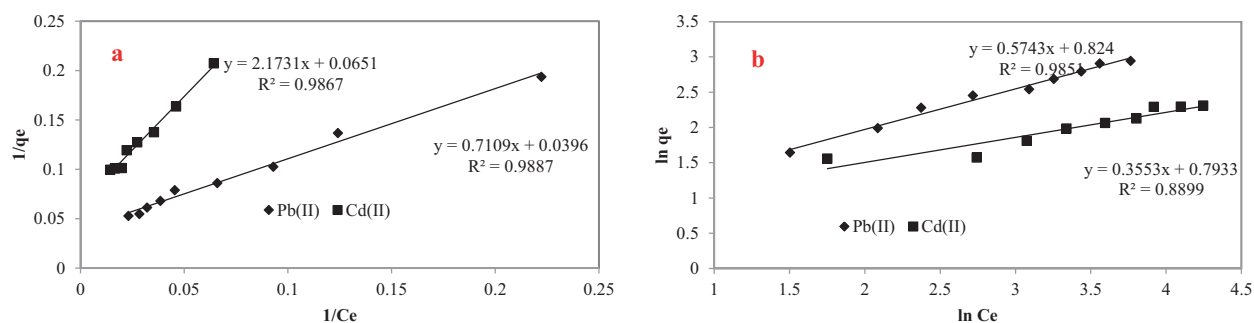
Figure 6. Pseudo-first-order (a) and pseudo-second-order (b) plots for Pb(II) and Cd(II) adsorption (pH $= 5$; C$_0 = 10$ mg L^{-1}; PSP dosage $= 0.3$ g, contact time $= 100$ min, temperature $= 20$ $^\circ$C).

chemisorption processes. Overall, the Langmuir isotherm model correlation coefficients were significantly closer to unity relative to those of the Freundlich isotherm model (Table 1). Moreover, the chi square values for the Langmuir model were lower relative to Freundlich, indicating that Langmuir isotherm model best fitted the experimental data. The maximum adsorption capacities of the adsorbent for Pb(II) and Cd(II) were 28.09 and 27.17 mg g^{-1}, respectively. Table 2 shows maximum adsorption capacities comparison between PSP and other adsorbents.

Table 2. Comparison with other adsorbents.

Metal ion	Sorbents	q$_{max}$ (mg g^{-1})	References
Cd(II)	Akagabeite nanocrystals	17.10	[24]
	Fe$_3$O$_4$@APS@AA-co-CA MNPs	29.60	[25]
	SDS modified magnetite nanoparticles	9.60	[26]
	Fe$_3$O$_4$/cyclodextrin polymer	27.70	[27]
	PSP	27.17	This study
Pb(II)	Maize stover	19.65	[15]
	Baobab fruit shell	7.65	[28]
	Maize stover	19.65	[2]
	PSP	28.09	This study

3.1. Adsorption kinetics

The adsorption kinetics was investigated using two kinetic models, Lagergren's pseudo-first-order model and Ho and Mckay's pseudo-second-order model.

The pseudo-first-order kinetic model is expressed in linear form as

$$\log (q_e - q_t) = \log q_e - \frac{t.k_1}{2.3} \tag{4}$$

where q$_e$ and q$_t$ are the amount of M(II) adsorbed (mg g^{-1}) onto PSP at equilibrium and at any time t, respectively, k$_1$ (min^{-1}) is the pseudo-first-order kinetic model rate constant, and t is the time (min). A plot of log (q$_e -$ q$_t$) versus t gave the values of k$_1$ from the slope and q$_e$ from the intercept. The results for the pseudo-first-order kinetic model are presented in Figure 7a and Table 3. The correlation coefficient values were found to be unsatisfactory (R^2 < 0.98), indicating that the kinetic model may not be suitable to describe the kinetics of M(II) adsorption onto PSP.
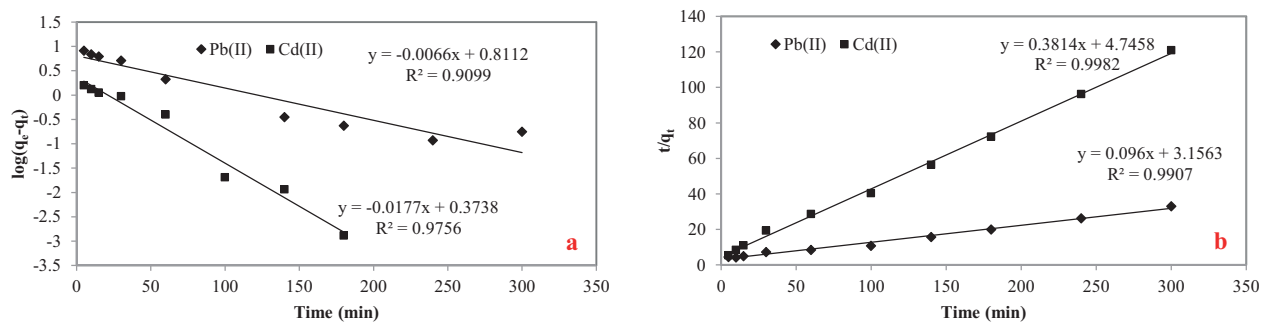
Figure 7. Langmuir isotherm (a), Freundlich isotherm (b) for Pb(II) and Cd(II) adsorption (pH = 5; PSP dosage = 0.3 g, contact time = 100 min, temperature = 20 °C).

Table 3. Kinetic parameters.

Metal ion	Experimental value	Pseudo-first-order kinetic model				Pseudo-second-order kinetic model			
	q_e (mg g^{-1})	q_e (mg g^{-1})	k_1 (min^{-1})	SSE	R^2	q_e (mg g^{-1})	k_2 (g mg^{-1} min^{-1})	R^2	SSE
Pb(II)	9.24	6.474	0.0152	0.859	0.909	10.417	0.0029	0.991	0.969
Cd(II)	2.492	2.365	0.0407	0.808	0.976	2.622	0.307	0.998	0.477

The kinetic data were further analysed using the pseudo-second-order model. The kinetic model is presented in the linear form as follows:

$$\frac{t}{q_t} = \frac{t}{q_e} + \frac{1}{k_2(q_e)^2} \tag{5}$$

where k_2 is the rate constant at equilibrium (g mg^{-1} min^{-1}). The values of k_2 and q_e were estimated from the intercept and slope of the plot of (t/q_t) versus t, respectively (Figure 7b). The adsorption pseudo-second-order kinetic data are presented in Table 3. The pseudo-second-order kinetic model correlation coefficients are all close to unity (R^2 > 0.98), suggesting the suitability of the model to explain the kinetics. Furthermore, the $q_{e,cal}$ value (mg g^{-1}) was found to be in better agreement with the $q_{e,exp}$ value (9.61 mg g^{-1}) relative to those of the pseudo-first-order kinetic model.

3.2. Adsorption thermodynamics

To understand the thermodynamic behaviour of the M(II) adsorption onto PSP, thermodynamic parameters such as standard Gibb's free energy change ($\Delta G°$), entropy change ($\Delta S°$), and enthalpy change (ΔH°) were calculated from the following equations:

$$\Delta G^o = -RT \ln K_c \tag{6}$$

$$K_c = \frac{q_e}{C_e} \tag{7}$$

$$\Delta G^o = \Delta H^o - T\Delta S^o \tag{8}$$

$$\ln K_c = \frac{\Delta S^o}{R} - \frac{\Delta H^o}{RT}, \tag{9}$$

where R is the ideal gas constant, T is the temperature (K), and K_c is the thermodynamic equilibrium constant. q_e is the equilibrium amount of M(II) adsorbed (mg L^{-1}) and C_e is the concentration of M(II) ions in solution at equilibrium. The slope and intercept of the van't Hoff plots (ln K_c versus 1/T) were employed to estimate the ΔH° and ΔS° values, respectively. ΔG° values were calculated to be –6.35, –7.09, –7.83, and -8.57 kJ mol^{-1} for Pb(II) and –5.97, –6.64, –7.731, and –7.98 kJ mol^{-1} for Cd(II) at 293, 303, 313, and 323 K, respectively. The Gibbs free energy values obtained were all negative, confirming the feasibility and spontaneity of the process. The incremental negativity of ΔG° with increase in temperature (Table 4) indicates that the adsorption process was favourable at higher temperature. The entropy and enthalpy change values were positive for both metal ions, showing formation of more chaotic solid/solution interface, whilst the positive ΔH° values show the endothermic behaviour of the adsorption process.

Table 4. Thermodynamic parameters.

Metal	Temperature (K)	ΔG° (kJ mol^{-1})	ΔH° (kJ mol^{-1})	ΔS° (kJ mol^{-1})
Pb(II)	293.15	–6.353	+15.430	+0.074
	303.15	–7.093		
	313.15	–7.833		
	323.15	–8.573		
Cd(II)	293.15	–5.971	+13.67	+0.067
	303.15	–6.641		
	313.15	–7.311		
	323.15	–7.981		

3.3. Desorption studies

The desorption results of Pb(II) and Cd(II) by using HCl solution are presented in Figure 8. Desorption studies were conducted to determine the regeneration potential of regenerating the spent adsorbent using 0.05, 0.1, 0.2, 0.3, 0.4, and 0.5 M HCl eluent. The desorption efficiencies of M(II) were enhanced as the HCl concentration was increased from 0.05 to 0.2 M (Figure 8). The maximum desorption of Pb (92.1%) and Cd (51.9%) was achieved with 0.2 M HCl. Beyond 0.5 M HCl concentration, there was a slight decrease in the desorption efficiency. Hence 0.2 M HCl was used in the subsequent adsorption–desorption studies. Six test cycles were carried out to investigate whether the PSP could be recycled. The Pb(II) removal efficiency of the adsorbent decreased from 92.1% (cycle 1) to 50.08% (cycle 6), whilst the Cd(II) removal efficient decreased from 51.9% (cycle 1) to 36.89% (cycle 6).
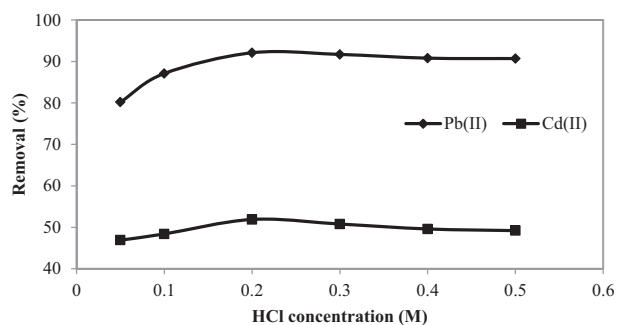

Figure 8. Desorption of Pb(II) ions from PSP.

3.4. Characterisation of the adsorbent

Figure 9 shows the FTIR spectra for the adsorbent (a) before adsorption and after (b) Pb(II) and (c) Cd(II) adsorption. A shift in the spectrum peaks, the disappearance and reduction of peaks, is used to determine whether the adsorbent influenced M(II) adsorption. The absorption band at 1093 cm^{-1} is a characteristic peak of the SiO$_4^{2-}$ group due to Si–O–Si symmetric stretching vibration.[30] The bands at 834 cm^{-1} and 556 cm^{-1} can be attributed to Si–O–Si bond bending vibrations. The peak at 3449 cm^{-1} is due to a hydroxyl group and the band at 1619 cm^{-1} is due to the bending vibrations of the H–O–H bond.[29]
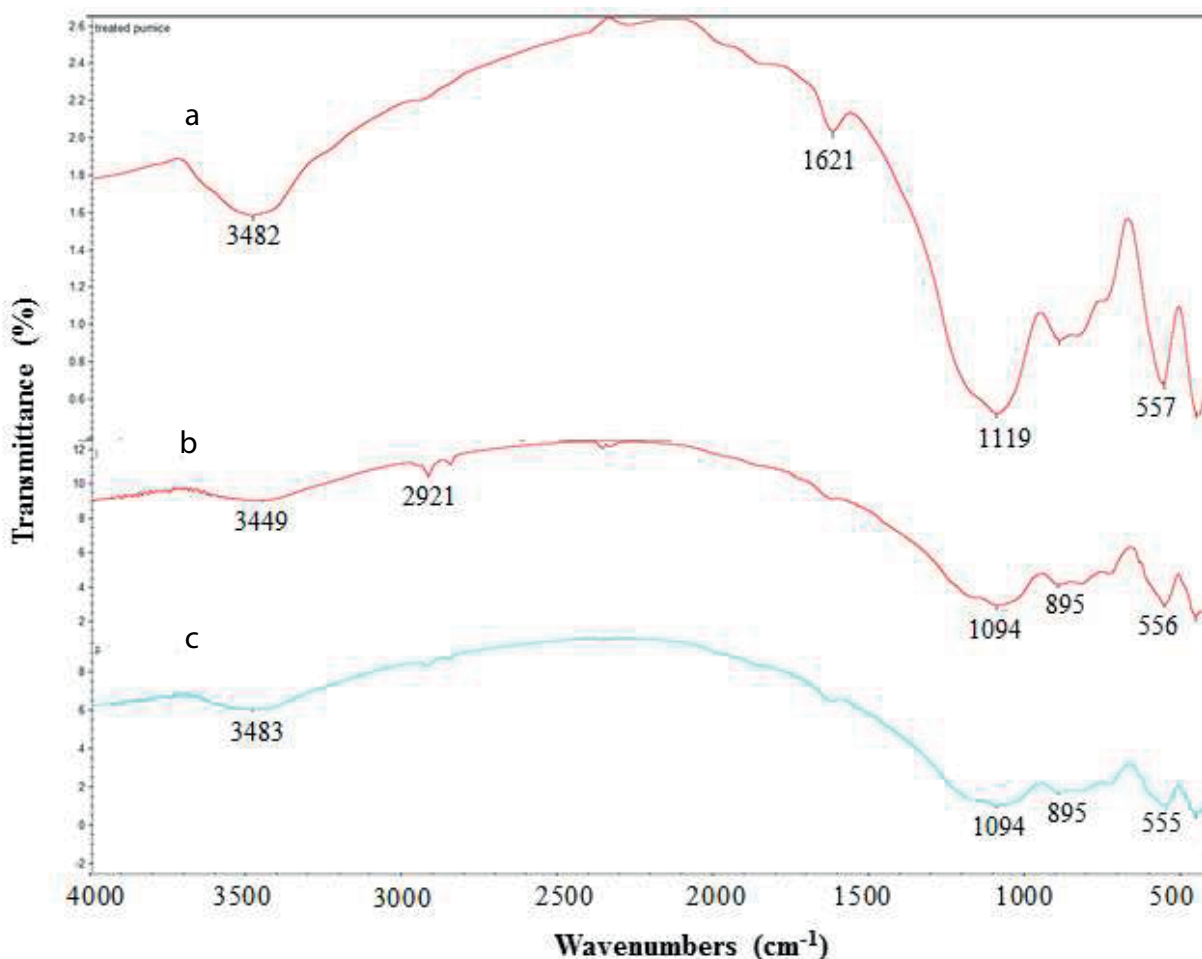

Figure 9. FTIR spectra of PSP: before (a) and after (b) Pb(II) and (c) Cd(II) adsorption.

The present study reveals that PSP has great potential as an adsorbent for the removal of Pb(II) and Cd(II) from aqueous solution. The Langmuir adsorption isotherm provided the better fit of the experimental sorption data for the Pb(II) and Cd(II) ions with maximum sorption capacities of 28.09 and 27.17 mg g^{-1}, respectively. The kinetic data were well described by the pseudo-second-order model with correlation coefficient (R^2) of 0.991 for Pb(II) and 0.998 for Cd(II). $\Delta S°$, $\Delta G°$, and $\Delta H°$ showed that the process was spontaneous, feasible, and endothermic. The loaded adsorbent was regenerated using 0.2 M HCl.

4. Materials and methods

4.1. Preparation of adsorbent

Pumice stones were obtained from Mutare, Zimbabwe. The collected pumice stones were washed with tap water several times followed by distilled water before being soaked in 0.1 M HCl to remove acid soluble impurities. Excess acid was removed by further washing several times with distilled water. Drying at 55 °C in an oven for 24 h removed most of the moisture. The dried stones were crushed to powder, which was further treated with 0.1 M NaOH for 24 h. The alkaline-treated material was oven dried at 55 °C for 72 h, crushed, and sieved through a 180-μm sieve.

4.2. Preparation of metal ion solutions

Stock solutions of Pb(II) and Cd(II) ions were prepared from pure analytical grade $Pb(NO_3)_2$ and $Cd(NO_3)_2$ by weighing 1.5987 g and 2.1 g, respectively, into separate 1000-mL volumetric flasks and topping up to the mark with distilled water. The solutions were stirred to obtain homogeneous stock solutions. Different concentrations of the metal solutions were prepared by serial dilution of the stock solutions. pH was measured using a Crison 2001 micropH (Spain). pH of the solution was adjusted using either 1 M HNO_3 or 1 M NaOH.

4.3. Adsorption experiments

The adsorption efficiency of pumice stone powder (PSP) for Pb(II) and Cd(II) ions was investigated with respect to pH in the range of 2–8. Briefly, 10 mg L^{-1} of Pb(II) and 10 mg L^{-1} of Cd(II) were placed in separate 250-mL flasks, and to it 0.2 g of PSP was added. The flask contents were agitated using a shaker at 150 rpm for 120 min at 20 °C.

For investigating the influence of dosage, 10 mg L^{-1} Pb(II) and 10 mg L^{-1} Cd(II) were placed in separate 250-mL flasks. Different PSP dosages ranging from 0.1 to 1.5 g were added. The flask contents were agitated on the shaker at 150 rpm for 120 min at 20 °C.

The effect of contact time was studied by placing 10 mg L^{-1} Pb(II) and 3 mg L^{-1} Cd(II) in separate 250-mL flasks. PSP (0.3 g) was added to each flask. The flask mixtures were agitated at 150 rpm for specified durations (5 to 300 min) at 20 °C.

For initial metal concentration, different Pb(II) (10 to 50 mg L^{-1}) and Cd(II) (1 to 5 mg L^{-1}) ion concentrations were placed in 250-mL Erlenmeyer flasks. Then, to each flask, 0.3 g of PSP was added followed by mechanical agitation at 150 rpm for 100 min for Pb(II) and for 140 min for Cd(II) at 20 °C.

The temperature influence was investigated in the range 20–50 °C for both metal ions. After mechanical agitation during study of the effect of each parameter, the mixtures were filtered through Whatman number 42 filter paper. The filtrates were analysed by atomic absorption spectrometer (Shimadzu AA-140, Japan). The metal ions percentage removal was calculated according to Eq. (1):

$$R = \frac{(C_o - C_e)}{C_o} \times 100\% \tag{10}$$

The amount of metal adsorbed by the adsorbent was calculated using Eq. (2):

$$q_e = \frac{(C_o - C_e)\,V}{M}, \tag{11}$$

where q_e (mg g^{-1}) is the amount of Pb(II) or Cd(II) adsorbed by PSP, C_0 and C_e are the metal concentrations (mg L^{-1}) in the solution initially and after adsorption, respectively, V is the volume (L) of the solution, and m is the mass (g) of adsorbent used in the experiment.

4.4. Error analysis

The chi square (χ^2) tests were adopted to determine the suitability of the isotherm model with respect to the experimental data. The χ^2 equation is as follows:

$$\chi2 = \sum \frac{(q_e - q_{e,m})^2}{q_{e,m}} \tag{12}$$

where q_e (mg g^{-1}) is the experimental equilibrium capacity and $q_{e,m}$ (mg g^{-1}) is the equilibrium capacity obtained from the model.

4.5. Desorption studies

PSP (0.6 g) was added to a 250-mL Erlenmeyer flask containing 100 mL of M(II) ions at a solution pH of 5.0 and solution temperature of 20 °C. The mixture was shaken at 150 rpm for 100 min. Thereafter, the adsorbent was filtered and used for desorption studies. The filtrate was analysed on FAAS for M(II) concentration to determine the amount adsorbed onto the adsorbent. In the desorption experiments, 50 mL of different HCl concentrations was added to the filtered and preweighed adsorbent. The mixture was shaken at 150 rpm for 100 min at 20 °C. The adsorbent was then filtered and the filtrate analysed for the desorbed Pb(II) ions concentration. The adsorption–desorption cycles were repeated six times by treating the adsorbent used with a preoptimised eluent (HCl) concentration (0.2 M).

References

1. Samarghandi, M. R.; Zarrabi, M.; Sepehr, M. N.; Amrane A, Safari, G. H.; Bashiri, S. *Iran. J. Environ. Healt. Sci. Eng.* **2012**, *9*, 9.

2. Wang, L.; Zhang, J.; Zhao, R.; Li, Y.; Li, C.; Zhang, C. *Bioresour. Technol.* **2010**, *101*, 5808-5814.

3. Baghapour, M. A.; Ranjbar, M.; Derakhshan, Z.; Faramarzian, M. *AWERProcedia Advances Appl. Sci.* **2013**, *1*, 139-145.

4. Belova, T. P.; Selivanova, O. N. *J. Environ. Sci. Eng.* **2012**, *1*, 514-521.

5. Ji, K.; Kim, J.; Lee, M.; Park, S.; Kwon, H.; Cheong, H.; Jang, J.; Kim, D.; Yu, S.; Kim, Y.; et al. *Environ. Pollut.* **2013**, *178*, 322-328.

6. Kalkan, E.; Nadaroglu, H.; Dikbas, N.; Tasgin, E.; Celebi, N. *Pol. J. Environ. Stud.* **2013**, *22*, 417-29.

7. Anayurt, R.; Sari, A.; Tuzen, M. *Chem. Eng. J.* **2009**, *151*, 255-261.

8. Alidoust, D.; Kawahigashi, M.; Yoshizawa, S.; Sumida, H.; Watanabe, M. *J. Environ. Manage.* **2015**, *150*, 103-110.

9. Dekhil, A.; Hannachi, Y.; Ghorbel, A.; Boubaker, T. *Chem. Eco.* **2011**, *27*, 221-234.

10. Kumar, P. S. *Environ. Prog. Sustain. Energ.* **2013**, *33*, 55-64.

11. Mubarak, N.; Daniel, S.; Khalid, M.; Tan, J. *Int. J. Chem. Environ. Eng.* **2012**, *3*, 1-4.

12. Paulino, A.; Santos, L.; Nozaki, J. *React. Funct. Polym.* **2008**, *68*, 634-642.

13. Saleh, T.; Gupta, V. K. *Environ. Sci. Pollut. Res.* **2012**, *19*, 1224-1228.

14. World Health Organisation. *Guidelines for Drinking-water Quality.* **2006**, 1.

15. Guyo, U.; Mhonyera, J.; Moyo, M. *Process Saf. Environ. Prot.* **2014**, *93*, 192-200.

16. Yavuz, M.; Gode, F.; Pehlivan, E.; Ozmert, S.; Sharma, Y. C. *Chem. Eng. J.* **2008**,*137*, 453-461.

17. Derakhshan, Z.; Baghapour, M.A.; Ranjbar, M. *Healt. Scope.* **2013**, 2, 136-144.

18. Moyo, M.; Chikazaza, L.; Nyamunda, B. C.; Guyo, U. *J. Chem.* **2013**, *2013*.

19. Guler, U.; Sarioglu, M. *J. Environ. Healt. Sci. Eng.* **2014**, *12*, 79.

20. Moyo, M.; Nyamhere, G.; Sebata, E.; Guyo, U. *Desalin. Water Treat.* **2014**, 1-11.

21. Sari, A.; Tuzen, *M. J. Hazard. Mater.* **2008**, *160*, 349-355.

22. Langmuir, I. *J. Am. Chem. Soc.* **1918**, *40*, 1361-1403.

23. Freundlich, H. M. *J. Phys. Chem.* **1906**, *57*, 384-470.

24. Deliyanni, E. A.; Matis, K. A. *Sep. Purif. Technol.* **2005**, *45*, 96-102.

25. Ge, F.; Li, M-M.; Ye, H.; Zhao, B-X. *J. Hazard. Mater.* **2012**, *211-212*, 366-372.

26. Bahrami, M.; Brumand-Nasab, S.; Kashkooli, H.; Firouzi, A. F.; Babaei, A. *Iran J. Healt. Environ.* **2013**, *6*, 221-232.

27. Badruddoza, A. Z. M.; Shawon, Z. B. Z.; Tay, W. J. D.; Hidajat, K.; Uddin, M. S. *Carbohydr. Polym.* **2013**, *91*, 322-332.

28. Chigondo, F.; Nyamunda, B. C. *IOSR J. Appl. Chem.* **2013**, *5*, 43-50.

29. Moyo, M.; Guyo, U.; Mawenyiyo, G.; Zinyama, N. P.; Nyamunda, B. C. *J. Ind. Eng. Chem.* **2015**, *27*, 126-132.

30. Sepehrl, M.; Mansur, Z.; Hossein, K.; Abdeltif, A.; Kamiar, Y.; Hamid, R. G. *Appl. Surf. Sci.* **2013**, *274*, 295-305.